Hydro-Magnetic Catalist and Quantillium: A New Experimental Approach to Qualia

Carlino Christian Francesco
No affiliations
fcnicolar@gmail.com

Abstract

Following work deals with the realization of an experimental setup, called Hydro-Magnetic Catalyst (HMC), which has allowed to provide early experimental results useful for the study of the origin of consciousness and subjective experience.
Experimental results demonstrate that:
- interactions between vicinal water and magnetic fields, oscillating with frequency in theta, alpha beta and gamma range, are fundamental for the qualitative perception of stimuli from the external environment (qualia). This perception can be measured by means of a new index called Quantillium (Ql)
- neurons and neuronal networks are not the repositories of consciousness and subjective experience. They constitute the information decoding hardware. This decoding is mostly digital, but passive properties of neuronal cells and their interconnections allow for a digital-to-analog reconversion of the signal. Analog signal could be responsible for broadcasting of information to the aqueous environment and for the perception, during waking state, of qualia and stream of consciousness.

Introduction

Consciousness is actually one of the great mistery of the universe and its unveiling has involved many scholars and even some Nobel laureate. But no theoretical approach has ever achieved experimental confirmation (Zeman, 2001).
Currently dominant position seems to be physicalism, according to which mental processes can be traced back to a set of physico-chemical processes that take place in the highly integrated neuronal networks of our brain.
According to functionalism, a more extreme form of physicalism, any Artificial Entity (AE) with a certain degree of complexity (number of processing units and of inerconnections between them) and programmed with specific algorithms, should manifest some form of consciousness, regardless of the matter it is made of (Wahbeh et al., 2022).
Nevertheless, failure of computer and cybernetic sciences in the development of an AE endowed with consciousness or subjective experience, is evident.
Extremely intelligent machines have been created, but they actually represent the equivalent of logical schemes, devoid of any emotional and semantic content.
AE is not pleased with its result or frustrated by failure.
AE does not feel pain, hunger, fear of death; it does not tend to exceed its limits.
AE processes symbols and information, without any intentional semantic skill.
AE does not possess sensations, values, motivations and purposes.

AE is devoid of individuality; each unit can be replaced with another identical one.

Physicalism, and any other materialistic theory about consciousness, can't currently account for phenomenology; the subjective features of conscious experience that Philosophy defines as "Qualia".
Being conscious means to have some kind of pheomenology on its own.
So we can say that wherever there is experience there is phenomenology; and wherever there is phenomenology there is consciousness.
And, according to Nagel, "an organism has conscious mental states if and only if there is something it is like to be that organism" (Nagel, 1974).
Thus, in our brain (and also in animals brain) there must be a hidden "something" or process not yet known from wich phenomenology arises.
In previous works John R Searle postulates the existence of a Causal Power inside the physical structure of the brain, from wich qualia arise (Warfield, 1999).
Until now, this theory has been impracticable because is it not yet known what kind of physical phenomenon could be at the origin of the Causal Power.

Present work deals with an actual paradigm shift that no longer considers neurons and neuronal networks (of any complexity) as the repositories of subjective experience and consciousness.
In the author's opinion, it is quite evident that number of neurons and interconnections are not fundamental to explain the origin of subjective consciousness.
In the animal kingdom the brain of each species has a different and peculiar neuronal content (e.g. about 530 million cortical neurons for dogs, 250 million for cats and 16 billion for humans) but it is considered undeniable the presence of consciousness for many of them.
There are pathological conditions characterized by a marked reduction of the number of neurons (i.e. ischemic insults, traumatic events or large surgical resections) anyhow associated with an adequate level of consciousness. On the other hand, there are also pathological conditions characterized by the absence or marked reduction of the content of consciousness even in the presence of limited or focal neuronal damage.
The cerebellum has a higher number of neurons than the cerebrum, but is devoid of any "imprint" of consciousness.
It is noteworthy that anomalies or acquired lesions of large portions of the cerebellum do not compromise state of consciousness.
Following previous considerations neurons and networks are "downgraded" to simple "hardware" needed to process the informations that reach our senses and brains.
Absurdly, a brain deprived of consciousness can still act as an informations processor even though it is not able to attribute semantic, emotional and experiential meaning to what is perceived, as expected and described by Chalmers' argumentation about philosophical zombie (Chalmers, 1996).
Finally, it is notable how neurosciences and researches on the mystery of the mind and consciousness, have overlooked two peculiar clues:
1) 90% of the brain is made up of water.
2)The brain has an oscillating electromagnetic activity, with variable frequency and intensity, according to the state of awareness and consciousness .

Materials and Methods

Following work deals with the realization of an experimental setup called Hydro-Magnetic Catalyst (HMC) made up of the following elements (Fig.1):

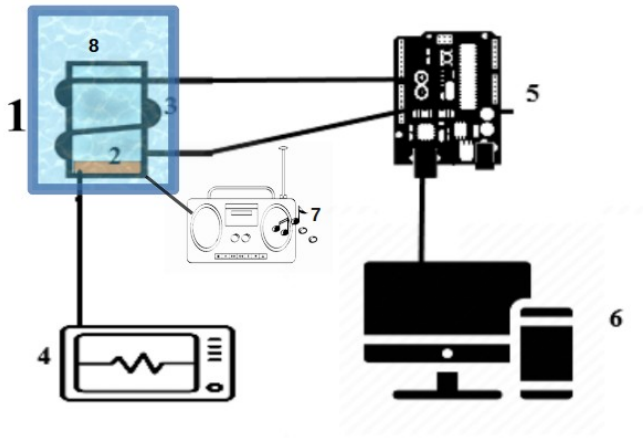

Fig.1: basic structure of HMC

- the exernal box filled with gelled water (1)
- the core (8) with the stimulation coil (2) and the external recording coil (3)
- the function generator (4)
- the microcontroller (5)
- the data processing and storage and spectral analysis system (6)
- the audio player (7)

Core

The Core is a 150cc glass container filled with gelled water. A copper coil (2) (10 coils of enamelled copper with R=2 cm) is immersed at the base of the container. Dimensions and number of turns of the coil have been calculated to generate, with current flow of about 30mA, an oscillating magnetic field with an intensity of a few microT (10-20 microT)

The external surface of the core has been covered with 100 coated copper turns: the recording coil (3).

Function Generator

The stimulation coil of the Core is connected to a wave function generator (4) (FeelTech FY3200S Dual Channel) that can be set in order to obtain an oscillating magnetic field with sinusoidal waves of desired frequency.

Microcontroller and ADC

Microcontroller embedded in HMC is an Arduino Uno board. This microcontroller can convert any analog information detect in the core environment into digital format and transfer it to a PC for mathematical processing and storage.

Microcontroller has been programmed in C and connected to the coil on the external surface of the core (registration coil - 3).

Signal processing system
PC is used ro record and processed signals sent by the microcontroller, for spectral analysis and to program microcontroller.

Audio Player
The Audio Player is directly connected to the stimulation coil and has been used to give musical input or noise input to the core.

Vicinal Water
In recent years, studies and experiments conducted by Prof Gerald Pollack about the characteristics of water, strongly demonstrated that properties of water contained in tissues of living organisms (vicinal water) are quite different from those of bulk water (Pollack, 2013).
In proximity to organic, hydrophilic surfaces, which tend to be negatively charged, water molecules organize themselves in such a way as to create a layer of negative charges in contact with the organic surface, creating an excess of remote positive charges in the bulk water.
Furthermore, separation of positive and negative charges in the interstitial water volume actually means that, in presence of oscillating magnetic fields, movements of these electrical charges can occur, due to the effect of Faraday's law, and if these moving charges cross the internal surface of a coil they can induce a measurable Electromotive Force.

Microcontroller Configuration and code (Appendix 1)
Microcontroller Arduino Uno has been programmed in cycles of 10000 loops of 1 msec each. Microcontroller has also been programmed with a sum algorithm increasing by one every time a valid action potential is perceived (line...set threshold value) and thus returning a total every 10000 detection loops (= 1 Cycle).
Microcontroller has also been endowed with a pseudo-RNG (Random Number Generator) whose starting seed is provided by the potentials detected by the recording coil (see line...).
RNG has also been set to generate only two results, 0 or 1, and to sum them. In case of pure randomness, at he end of each cycle (10000 samplings), the sum will be approximately *5000 (5000 numbers 1 and 5000 numbers 0) and this represented the null hypothesis of the chi-square test that has been used to evaluate the statistical significance of the deviation from pure randomness.*
The greater the deviation from this value, the greater the statistical significance of the non-random nature of the result.
To sum up: every 10 sec (10000 loops = 1 Cycle = 10000msec) microcontroller returns the sum of 10000 detections (S-POT) where, in case of potential above threshold number returned is 1 otherwise the number returned is 0 (e.g. if the number of potentials above threshold 0 is 50% the microcontroller will return the number 5000). Each loop restarts after 10 msec.
At the end of each cycle microcontroller returns also other variables: Total Power of the system (TP), Power Above Threshold (PAT), Power Below Threshol (PBT), Total RNG (tRNG) and Deviation from Randomness (Δ).
To obtain a statistically significant data set for each experiment, 50 consecutive cycles were taken in order to obtain $5*10^5$ detections every 10 min approximately.

Frequencies

Electromagnetic activity of the brain has very different frequencies, ranging from 0.5 Hz to 100Hz
There are several classes of brain wave frequencies that are associated to different brain states ((John, 2002).

Delta Waves (0.5 Hz – 3.5 Hz)
They are found most in the deepest levels of sleep.

Theta Waves(3.5 Hz – 7.5 Hz)
Theta waves helps in creativity, emotional connection, intuition, and relaxation.

Alpha Waves(7.5 Hz- 12.5 Hz)
Alpha waves promote feelings of deep relaxation. When they are optimal it leads to a relaxed state.6

Beta Waves(12.5 Hz – 25 Hz)
Beta waves are commonly observed in an awaken state. They are involved in conscious thought, logical thinking and attention focusing.

Gamma Waves(25 Hz – 100 Hz)
Gamma waves are associated to cognitive functioning, focus, perception and binding of senses (smell, sight and hearing), learning, memory, and information processing.

In present work following frequencies of stimulation has been employed: 3 Hz (delta), 5Hz and 7Hz (theta), 8 Hz (alpha), 13Hz and 21Hz (beta), 34 Hz, 55Hz and 89 Hz (gamma), over 100 Hz (non-physiological stimulation).

Results

a) Causal Power

First of all the HMC was tested in with / without water and with / without oscillating magnetic field. Results are reported below.

1) Without H_2O microcontroller does not detect any information, both with or without oscillating magnetic field.

2) With H_2O and oscillating magnetic field, microcontroller detects rather chaotic potentials, probably related to the movement of charges in the aqueous medium and through the inner surface of the coil 3.

Graphs 1,2 and 3 show the variation of number of potentials detected at different threshold (>5mV, >25 mV, >50 mV), under the same frequency of stimulation (8Hz), in three samples of water: demineralized water (H2O), physiological solution (PS) and gelled physiological solution (8% solution of cornstarch) (PSG).

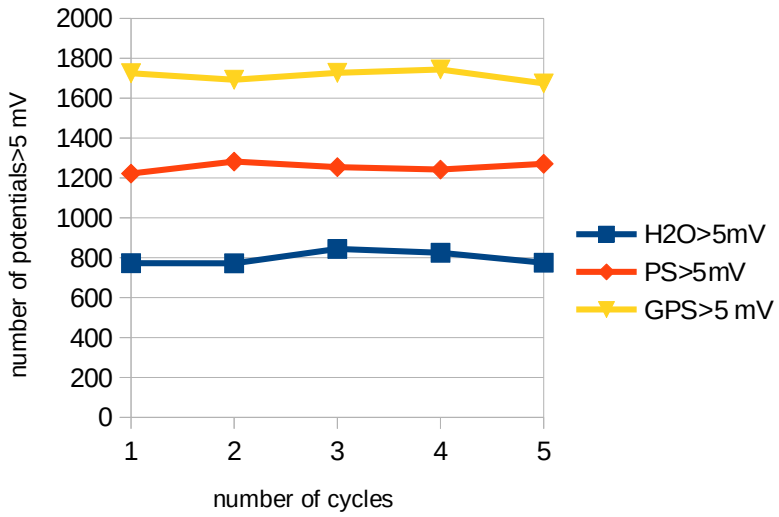

Graph 1: Number of potentials > 5mV in various samples of water (8Hz stimulation)

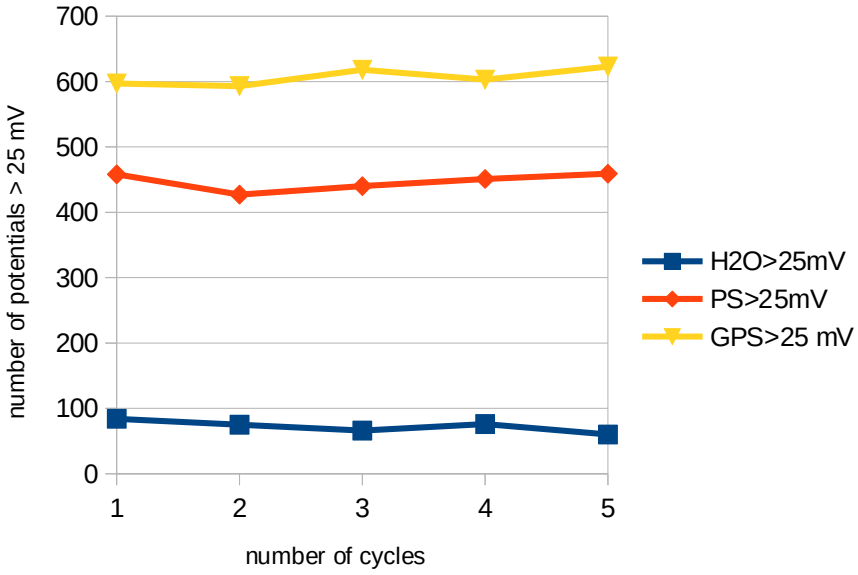

Graph 2: Number of potentials > 25mV in various samples of water (8Hz stimulation)

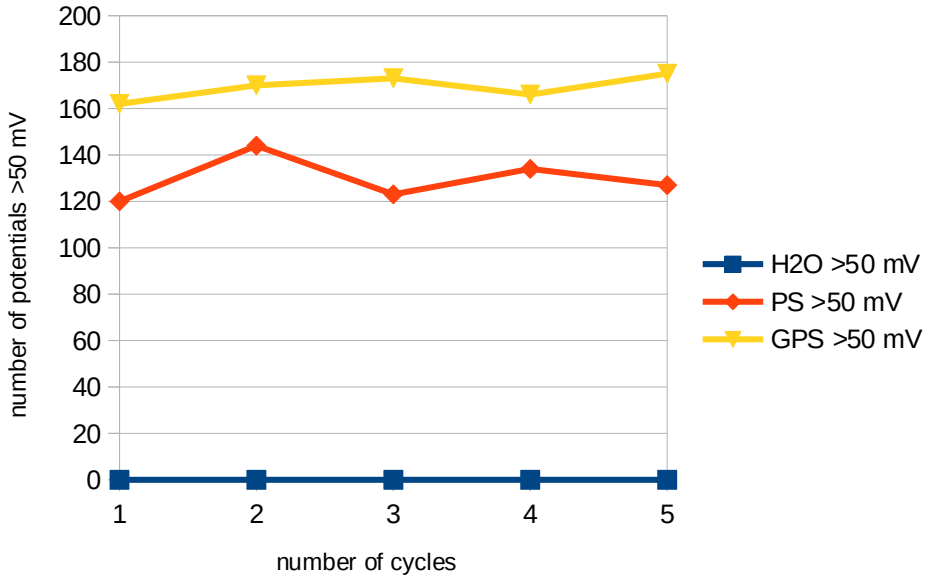

Graph 3: Number of potentials > 50mV in various samples of water (8Hz stimulation)

Regardless of threshold, number of potentials actually increases when water samples are supplemented with salts (PS) and, according to Pollack, when they are gelled(PSG).

It is also interesting to note that only stimulation with oscillating magnetic fields can induce potentials. If we remove oscillating magnetic field and replace it with a less coherent magnetic fields generated by stimuli of different nature (e.g. noise or music), also applied through the stimulation coil, number of detected potentials does not undergo significant variations compared to baseline (no input) (Graph.4).

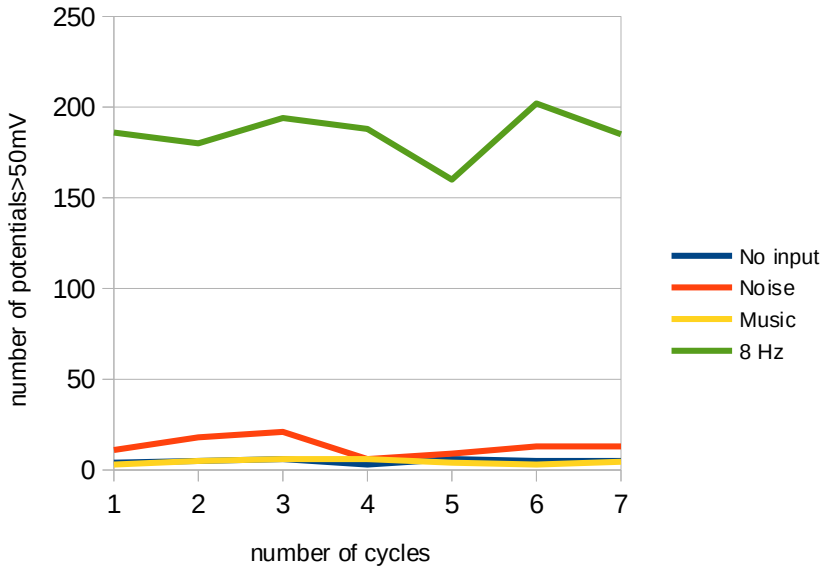

Graph.4: detected potentials >50mV with different kind of stimulations

These results actually show an emergent property of the HMC system, a source of power that appears only after the interaction between coherent oscillating magnetic fields and the aqueous environment.
In agreement with Searle's hypotheses, this property has been defined Causal Power (CP).

b) Causal Power Index
After defining CP as an emergent property of the HMC, it is necessary to ask how this property could behave during the application of sensory inputs of different nature and for stimulation frequencies included in the Delta – Gamma range.

In other words, the main question of the following work is: is there any perturbation of the HMC system that correlates with the different phenomenological characteristics of sensory inputs and could therefore represent the biophysical singularity at the origin of qualia?

To answer this question HMC and CP responses have been tested varying potential threshold (25mV and 70mV), stimulation frequency (from 3 Hz until 144 Hz) and features of analog input signal.
Since literature suggests that presence of sound results in a more pronounced brain activity (Farabbi et al., 2022) two different audio input have been chosen:
- Music: Chopin Grand Polonaise Brilliant for piano and orchestra
- Noise: radio white noise.

These kind of sensory input, each one converted to different electomagnetic field by the stimulation coil, are very different both on the objective physical level (power spectrum and spectral analysis) and on phenomenological level (one pleasant, the other annoying), so as to be able to induce different, and more easily identifiable, system behaviors.

As an example Tables 1 and 2 report (respectively for potential thresholds of 25mV and 70mV) variable data obtained for a stimulation frequency of 8Hz without input.

TAB 1: 8 Hz stimulation; Power Threshold = 25mV

S-POT	TP	PAT	PBT	RNG	Δ
808	13215	11035	2180	4886	114
811	13474	11354	2120	4944	56
825	13537	11254	2283	4919	81
798	13388	11185	2203	5040	-40
828	13791	11575	2216	4964	36
823	13460	11383	2077	4978	22
827	13402	11281	2121	4946	54
873	13989	11905	2084	4992	8
824	13726	11351	2375	5032	-32
818	13425	11206	2219	5000	0
833	13827	11523	2304	4907	93
797	13396	11149	2247	4874	126
828	13812	11551	2261	4969	31
785	13465	11105	2360	4946	54
829	13905	11637	2268	4943	57
858	13821	11592	2229	4910	90
796	13217	10983	2234	4910	90
850	13869	11656	2213	4981	19
808	13342	10968	2374	4905	95
793	13081	10648	2433	5013	-13
833	13881	11725	2156	4820	180
789	13212	10857	2355	4964	36
799	13244	11095	2149	4944	56
769	12892	10577	2315	4964	36
823	13526	11368	2158	4901	99
777	12655	10571	2084	4966	34
804	13100	10923	2177	5017	-17
802	13461	11290	2171	4979	21
812	13455	11148	2307	4971	29
807	13394	11185	2209	4968	32
806	13389	11122	2267	4910	
822	13512	11218	2294	5021	-21
796	13313	11003	2310	4888	112
808	13469	11226	2243	4904	96
821	13405	11279	2126	4898	102
781	13014	10890	2124	5032	-32
791	13322	11106	2216	4952	48
830	13462	11300	2162	4909	91
757	12435	10244	2191	4965	35
833	13596	11346	2250	4953	47
797	13472	11212	2260	5004	-4
819	13265	11114	2151	4866	134
822	13405	11244	2161	4946	54
806	13155	10973	2182	4997	3
779	12622	10553	2069	4878	122
794	13055	10832	2223	5008	-8
827	13857	11483	2374	4967	33
838	13886	11585	2301	4980	20
816	13133	10949	2184	4917	83
824	13319	11153	2166	5034	-34

TAB 2: 8 Hz stimulation; Power Threshold = 70mV

S-POT	TP	PAT	PBT	RNG	Δ
357	14260	6995	7265	4967	33
397	14961	7807	7154	4951	49
368	13945	7176	6769	5042	-42
367	13998	7127	6871	4983	17
359	14099	7072	7027	4952	48
351	13902	6809	7093	4879	121
399	15160	7816	7344	5061	-61
341	13638	6697	6941	4991	9
345	13864	6722	7142	4968	32
361	14274	7180	7094	4978	22
349	14248	6942	7306	5041	-41
360	13922	7070	6852	4977	23
370	14575	7515	7060	4979	21
386	14780	7633	7147	4932	68
375	14447	7353	7094	5044	-44
399	15020	7817	7203	4965	35
373	14407	7125	7282	5047	-47
363	14191	7138	7053	4943	57
375	14722	7510	7212	4980	20
386	15088	7487	7601	4961	39
418	14940	8212	6728	5040	-40
428	15448	8415	7033	4958	42
386	14532	7558	6974	4859	141
365	13977	7096	6881	4956	44
354	14384	6985	7399	4979	21
358	13976	7039	6937	5051	-51
357	14471	6998	7473	4960	40
373	14526	7498	7028	4935	65
354	14764	7031	7733	5038	-38
370	14333	7178	7155	4978	22
349	14056	6829	7227	5028	-28
369	14627	7215	7412	4940	60
384	14999	7467	7532	4998	2
328	13709	6494	7215	4977	23
375	14638	7267	7371	4981	19
350	14091	6862	7229	4952	48
366	14235	7283	6952	5042	-42
374	14450	7376	7074	4960	40
363	14454	7072	7382	4967	33
360	14364	7104	7260	4978	22
355	14083	6955	7128	4972	28
365	13834	6987	6847	4985	15
386	14709	7584	7125	5001	-1
370	14449	7286	7163	5026	-26
364	14306	7179	7127	4887	113
352	13886	6887	6999	5007	-7
362	13900	7123	6777	4961	39
354	13913	7013	6900	4871	129
374	14668	7321	7347	4914	86
365	14128	7157	6971	5037	-37

Trends of each single variable obtained after each cycle have been related to each other obtaining sixteen different types of index called Causal Power Index (CPIx).

Table 3 reports the mathematical definition for each CPIx.

Tab.3: different types of CPIx

CPIx	FORMULA	DESCRIPTION
CPI_1	$\frac{((PBT)_n-(PBT)_{n-1})/(PBT)_{n-1}}{((PAT)_n-(PAT)_{n-1})/(PAT)_{n-1}}$	ratio between PBT variation and PAT variation between two consecutive cycles
$\lvert CPI_1 \rvert$		CPI_1 module
CPI_2	$\frac{((TP)_n-(TP)_{n-1})/(TP)_{n-1}}{((S\text{-}POT)_n-(S\text{-}POT)_{n-1})/(S\text{-}POT)_{n-1}}$	ratio between TP variation and S-POT variation between two consecutive cycles
$\lvert CPI_2 \rvert$		CPI_2 module
CPI_3	$\frac{((TP)_n-(TP)_{n-1})/(TP)_{n-1}}{((PAT)_n-(PAT)_{n-1})/(PAT)_{n-1}}$	ratio between TP variation and PAT variation between two consecutive cycles
$\lvert CPI_3 \rvert$		CPI_3 module
CPI_4	$\frac{((TP)_n-(TP)_{n-1})/(TP)_{n-1}}{((PBT)_n-(PBT)_{n-1})/(PBT)_{n-1}}$	ratio between TP variation and PBT variation between two consecutive cycles
$\lvert CPI_4 \rvert$		CPI_4 module
CPI_{-1}	$\frac{((PAT)_n-(PAT)_{n-1})/(PAT)_{n-1}}{((PBT)_n-(PBT)_{n-1})/(PBT)_{n-1}}$	ratio between PAT variation and PBT variation between two consecutive cycles
$\lvert CPI_{-1} \rvert$		CPI_{-1} module
CPI_{-2}	$\frac{((S\text{-}POT)_n-(S\text{-}POT)_{n-1})/(S\text{-}POT)_{n-1}}{(TP)_n-(TP)_{n-1})/(TP)_{n-1}}$	ratio between S-POT variation and TP variation between two consecutive cycles
$\lvert CPI_{-2} \rvert$		CPI_{-2} module
CPI_{-3}	$\frac{((PAT)_n-(PAT)_{n-1})/(PAT)_{n-1}}{(TP)_n-(TP)_{n-1})/(Tp)_{n-1}}$	ratio between PAT variation and TP variation between two consecutive cycles
$\lvert CPI_{-3} \rvert$		CPI_{-3} module
CPI_{-4}	$\frac{((PBT)_n-(PBT)_{n-1})/(PBT)_{n-1}}{(TP)_n-(TP)_{n-1})/(TP)_{n-1}}$	ratio between PBT variation and TP variation between two consecutive cycles
$\lvert CPI_{-4} \rvert$		CPI_{-4} module

The aforementioned procedure was applied to each stimulation frequency, to each power threshold and to each sensorial input; trends of the average value of each CPIx obtained at the end of the 50^{th} cycle, for each individual stimulation frequency (with and without input), are shown in Fig.2 and Fig.3.

FREQ	CPI_1	$\|CPI_1\|$	CPI_2	$\|CPI_2\|$	CPI_3	$\|CPI_3\|$	CPI_4	$\|CPI_4\|$	CPI_{-1}	$\|CPI_{-1}\|$	CPI_{-2}	$\|CPI_{-2}\|$	CPI_{-3}	$\|CPI_{-3}\|$	CPI_{-4}	$\|CPI_{-4}\|$
3HZ	-0,74528586	1,48526133	0,68864657	1,18136452	0,22271815	0,77588707	7,07742596	9,34274305	11,652226	16,9357903	1,25044303	5,36207274	2,2565524	4,65380448	-0,42822039	4,3832733
+mus	1,4505877	2,89361078	0,41304691	1,09228337	1,18546764	1,46901437	3,18978284	4,60227518	4,91176696	8,22967251	4,55494408	5,68483229	4,32206268	5,02018615	-3,20262949	5,82902345
+noise	5,04803057	8,67999985	0,56163888	1,0378026	2,75475617	4,30443087	1,51017941	2,57674121	2,04898875	5,00582368	1,57771089	2,45712754	1,76646296	2,36517731	0,21310617	2,00765262
5HZ	-0,6822559	1,10047715	0,36542814	0,69540294	0,21176254	0,65956487	1,44896701	3,28066104	1,77351902	6,34421177	3,09992711	3,58320745	4,73806687	5,28841818	-3,08542079	4,74804296
+mus	-0,13233646	0,61017388	0,53559599	0,82047255	0,46321402	0,52555243	-1,40346313	2,94866891	-3,55538876	5,93772049	-2,96982497	7,77853086	-7,80907977	13,431779	10,5157083	13,0424934
+noise	0,37721554	1,16284684	0,88096505	1,1919434	0,71109141	0,86789406	1,54016222	4,04201535	1,98630951	6,44800205	1,86392923	3,36578656	2,30099316	3,84883339	-0,50554012	2,93051309
7HZ	3,58638431	4,79506498	0,58854582	1,23223176	2,18660479	2,54554014	0,0767359	2,27738175	-0,70157793	3,96477011	0,66040417	2,45597895	1,19643084	2,40820453	0,65940618	2,20155884
+mus	1,34460877	2,9845427	0,44637089	0,99985748	1,11760239	1,67029509	0,60211702	2,12451251	0,25915055	3,93328106	1,38318329	3,11000532	1,74700954	2,69562672	0,18389144	2,11556761
+noise	-0,16471473	1,5467812	0,92425538	1,10625837	0,78797537	1,10312964	4,53309145	6,45030523	8,40891152	13,1708016	1,56353876	1,8060643	1,83417289	1,92805779	0,21852437	1,02377218
8HZ	4,32311099	5,59173689	0,48380978	1,07393094	2,29073251	2,5945508	1,14943153	1,55813709	1,28583379	2,71860972	-11,4769599	18,4834258	-8,87994522	16,2520705	11,6185813	17,4041839
+mus	0,32792126	2,11739336	0,76432175	0,98578552	0,63214815	1,21549097	-1,77706859	4,96458	-4,26535152	9,18705074	-1,49928804	5,55323349	-0,33983806	4,42963609	2,8607601	4,90300732
+noise	-1,54812681	2,38635952	0,13070742	0,9624197	-0,2372595	1,30254776	0,6533222	1,40779367	0,28672578	2,42956059	-0,81261226	5,35910637	-1,30142065	6,27685811	3,48198163	6,32221001
13HZ	-0,16611792	1,37903086	0,06785951	1,30164658	0,43296758	0,78676202	0,81561076	1,89978611	0,72478437	3,54025587	2,56010069	3,14546045	2,38955242	3,25775408	-0,32693312	2,89649067
+mus	-3,82255782	4,63135502	0,15408016	0,96000653	-1,25965424	2,38163172	0,4993047	1,30086713	0,06155365	2,42681221	0,84767047	2,5916276	0,93081321	2,84885824	1,01950891	2,55237756
+noise	-2,48011217	2,76393044	0,63938488	0,92843658	-0,77657647	1,50276507	0,3954803	2,81408833	-0,32480584	6,02231641	4,68318268	10,0024636	2,75526786	7,96698614	-0,33716508	6,70253158
21HZ	1,77590682	2,93568469	0,9037184	1,48082807	1,35032546	1,62752155	-0,0825052	2,78752436	-1,021325	5,11947944	0,72816491	3,1886416	0,78057414	2,97688464	1,30585263	2,8304212
+mus	-8,96405316	9,30153575	0,38071822	0,98141245	-3,65756238	4,6393595	2,93696045	4,29742612	4,67576366	8,24617704	-1,32448924	6,52485975	-1,44980699	5,9130736	3,64509029	5,7576379
+noise	-11,6926203	13,0783741	0,4568476	1,15964092	-5,22013107	6,79100687	-0,41453793	1,79159312	-1,9865779	3,80430258	1,00315628	3,0782871	1,14928559	3,12666769	0,78816364	2,34292953
34HZ	-0,34262041	1,56779546	0,66315839	0,87028014	0,31715498	0,97917531	0,30082648	1,80708583	-0,32849489	3,46776789	1,78627888	2,19315346	1,74498803	2,21228373	0,20635103	1,56603008
+mus	1,70680148	2,29339896	0,60545173	0,65874086	1,30138586	1,3715653	0,72471176	2,65335199	0,47899756	5,14407525	2,50817513	3,05569363	3,07232146	3,54616589	-1,2049864	2,89714549
+noise	-0,57252031	1,13585204	0,25486774	0,69008279	0,17682756	0,68136533	-8,46219487	10,8219293	-18,1602954	22,0227905	0,85130335	6,77381278	0,75008468	5,46100542	1,4598146	4,42160839
55HZ	0,58746178	1,60965736	0,43111556	1,20774674	0,81166598	0,95060854	-0,21622393	4,43086663	-1,23446764	8,27389711	-5,32726182	10,3562342	-1,78980954	7,12730773	3,98234147	7,0850793
+mus	-0,11878384	3,76580018	0,18940904	1,51530301	0,47803047	1,93646455	-0,16607545	1,67070967	-1,14558763	2,88185967	0,14137386	2,88923945	-0,04160624	3,28175852	2,50926637	3,79510136
+noise	0,0969404	1,38011299	0,9219574	1,36302863	0,47574543	0,93154165	2,23792353	3,31493822	3,38594903	6,44062071	11,484397	12,0114608	12,2733608	12,6045776	-10,3270765	11,9492407
89HZ	2,23714909	3,32398426	-0,2816295	1,70262939	1,41646496	1,49928305	11,4982507	13,8549928	17,5073413	22,129332	-4,9484059	11,229411	-4,5491150	10,3928738	8,47849506	14,4257819
+mus	-0,51437108	1,91024844	0,9257983	1,46931606	0,4350204	0,88358912	0,27797639	1,75324467	-0,20331361	2,87274429	3,2833801	4,04248048	3,84072784	5,18762585	-4,01896975	7,93296467
+noise	-0,02175969	2,11754774	0,57993879	1,02956023	0,36601192	1,13354045	-1,40332622	6,32351701	-3,27953749	10,9033427	0,59886245	2,43630428	0,31833232	3,11441585	2,13732121	3,36015736
144HZ	-0,03493482	2,15487001	11,1297008	11,438298	0,7155449	0,87791731	-1,3504315	2,79772481	-2,20927237	3,93038161	4,09423069	5,13475261	1,2908328	2,23118552	0,18611864	3,88561965
+mus	0,5524438	6,50819763	0,57414692	1,22001941	0,86200724	2,03757182	1,62256905	2,13741186	1,84544831	2,83943531	-0,40279322	4,21466938	1,82101296	2,55244518	-1,26865166	5,05769805
+noise	-1,34014625	2,96750044	0,15753366	1,15197342	0,49171802	1,19879878	-0,39990515	1,72711368	-0,99859268	2,54919194	0,86719532	1,92385912	0,22561286	2,74043146	2,63419274	4,54950077

Fig.2 CPIx – Threshold = 70mV

FREQ	CPI_1	$\|CPI_1\|$	CPI_2	$\|CPI_2\|$	CPI_3	$\|CPI_3\|$	CPI_4	$\|CPI_4\|$	CPI_{-1}	$\|CPI_{-1}\|$	CPI_{-2}	$\|CPI_{-2}\|$	CPI_{-3}	$\|CPI_{-3}\|$	CPI_{-4}	$\|CPI_{-4}\|$
3HZ	-0,89909367	3,81590066	0,2967453	1,57667544	0,78066485	1,0011158	-0,39631588	1,25282696	-0,59281085	1,44714648	0,35463298	2,78556924	1,03499115	1,55121172	0,74771956	5,97590256
+mus	1,04851665	3,65600282	-0,94704157	2,25844207	0,99716504	1,01457154	-1,43877335	2,98228417	-1,77433599	3,42344221	-6,20146834	11,2699973	0,68131367	2,26756091	4,08393378	11,375412
+noise	0,23547206	2,93987766	0,59767263	3,17725555	0,87098145	1,11485119	1,42642727	2,67389876	1,49342245	3,13604893	-3,42918482	5,17633999	-2,10863864	4,26062856	15,5107628	16,56678
5HZ	-0,01553692	4,5526965	1,37812567	1,78464881	0,92005323	1,11163275	-1,46401326	2,98300372	-1,79219198	3,38779008	0,48474354	2,10366178	0,90944865	1,46253144	1,6624788	5,65023543
+mus	-12,4784052	16,3653925	0,71446667	1,60448651	-0,42500515	2,59213936	3,42966365	4,23054165	3,76729049	4,8068171	0,63909089	1,72241884	0,94861554	1,16123927	1,38929179	3,67453654
+noise	0,47859135	2,47008198	1,0223234	1,42270735	0,85803792	0,94173761	0,58774166	1,31216487	0,50673477	1,55375018	1,4265279	2,41420688	1,34463108	1,52601655	-0,75128961	3,49661302
7HZ	-0,59782452	4,32367195	1,35091149	1,55808664	0,81293191	1,13553117	0,12517733	1,65789084	0,00865944	1,88962229	0,66726908	1,4064627	0,94561908	1,1149226	1,46855429	2,98741076
+mus	5,882383	23,350572	0,80780607	1,38350601	1,51140623	3,2091552	0,02419255	1,32694912	-0,1021397	1,50520438	0,81725579	2,16685625	0,95970136	1,35215889	1,15529942	5,42765029
+noise	-1,82559163	3,42140657	0,72171643	1,77991736	0,52088276	0,9743283	0,48845712	2,55776356	0,38812669	3,11257937	2,57657896	5,10205822	3,70173789	3,78801525	-12,6241624	14,3637367
8HZ	-0,21907023	1,58425793	1,5459676	1,85606373	0,83800175	0,83800175	-0,72083178	4,13425573	-0,98686599	4,8046384	1,43212819	1,45412063	1,48752093	1,48752093	-2,3220246	3,35618348
+mus	-0,22653851	5,50920026	-0,03934545	1,51734769	0,77635168	1,17951972	0,01661591	1,85392136	-0,11519634	2,0926202	2,46452465	4,43251328	1,21851498	2,03429362	-0,71257331	10,8590538
+noise	-0,44822888	2,23383245	0,70245458	1,23408784	0,73046975	0,84897179	0,00910893	2,35933786	-0,19135936	2,84005542	0,65448377	2,29388193	2,13451625	2,28183657	-4,73817776	7,40020035
13HZ	-20,2358789	22,0357637	0,43761538	1,64220388	-1,47478174	3,3392407	0,31158766	1,232869	0,20989537	1,38700251	1,21076352	1,32462486	1,12934087	1,16840365	0,1814387	2,60860638
+mus	-0,87073375	6,11302725	1,06491167	1,56495472	0,76455585	1,33802209	1,13355894	4,52097767	1,15686691	5,1678176	1,43334031	2,43601915	1,47588068	1,88220688	-2,802562	7,89735184
+noise	0,94544409	3,77585918	0,47438374	1,08461298	0,97562792	1,14464032	-0,04905352	2,16956878	-0,25803742	2,60360993	1,07765686	2,15304623	1,24679242	1,3680525	-0,17452661	3,09889159
21HZ	3,70351253	4,93869917	0,6414432	1,42611985	1,33939647	1,33939647	0,47172784	1,66086797	0,39731778	1,90117503	1,07258893	1,38788711	1,15913555	1,15913555	-0,09407539	2,25984332
+mus	-0,92794598	2,07545524	1,05614092	1,09087203	0,77151214	0,8587838	1,49665438	3,71489761	1,58412028	4,26353627	2,79472911	3,02130639	2,42475134	2,73381393	-8,13636167	12,3405693
+noise	0,0744596	2,76108385	1,17558993	1,99801894	0,83479506	0,92241099	1,2335865	1,94608135	1,27820967	2,37348911	1,51668897	3,19983758	1,36321425	1,90225877	-0,5205194	5,50902771
34HZ	1,06353475	3,12886129	1,16400621	1,24810388	1,0015144	1,00723836	0,64140819	1,80730416	0,59481305	2,07895516	1,68395874	1,93839314	1,62336316	1,91441543	-3,58161458	7,43258084
+mus	0,41846409	9,72670549	-1,50695587	3,77417848	0,9125243	1,84423354	1,5727945	3,20722706	1,66019185	3,64444524	-0,27220664	2,23291093	0,51056801	1,73835226	4,09477712	6,82871466
+noise	-2,06542572	4,94392824	1,04811948	2,28590219	0,45288403	1,34204651	2,69689061	5,59364249	3,03266468	6,77194942	0,84436785	1,7143291	1,33455876	2,66804139	-0,77192087	9,82402821
55HZ	-2,59411257	4,0708226	0,3911791	1,76588594	0,54348381	0,93346325	-0,12491328	3,03227149	-0,27684108	3,44011927	-1,74032416	3,38242865	1,03370269	1,94034013	0,36994003	9,15543362
+mus	-0,18330363	1,80287989	1,30603845	1,81830148	0,87068727	0,92030006	-2,26847971	3,38485932	-2,67275212	3,80907934	0,85047885	0,93155679	0,77832827	1,35879091	2,60653142	3,78415187
+noise	1,16749196	3,29316544	0,85849418	1,29745038	1,0217236	1,07705897	3,47020237	5,28025235	3,9958136	6,4281638	-2,50620045	4,68651298	-3,72471054	6,17908543	21,8908575	24,2586746
89HZ	-1,8772355	5,46010699	0,17793918	2,10533267	0,73765006	1,1347707	-0,001254	0,86363452	-0,11671643	0,97009104	0,98151865	1,99262102	1,04849949	1,23086157	0,47742632	4,48212588
+mus	2,42668907	5,44591768	2,38554443	2,72884977	1,14390355	1,22453408	-0,59859386	1,97523686	-0,76316475	2,18136886	-1,64327729	4,55931045	1,22670848	1,24737029	-1,25210285	4,48698152
+noise	-0,74685778	2,08937666	1,82178643	3,69551346	0,75712063	0,87378632	0,12851411	2,55335907	-0,00970404	2,98092943	1,25276073	1,81402645	1,04411423	1,48728854	0,35120076	3,48544022
144HZ	-4,09452446	7,47407913	1,03483887	1,55677349	0,62287398	1,11690018	-0,27365047	1,33203235	-0,36313941	1,42559989	-0,04137819	2,38566652	0,94556642	1,15461335	1,83054971	5,76024151
+mus	5,5554763	8,83123838	-0,45790987	2,08317692	1,27722837	1,27722837	0,26789736	1,32800012	0,21844239	1,42404165	-9,31738654	12,778251	2,53834271	2,53834271	-22,3871226	27,3634896
+noise	-0,53408838	2,59461905	0,04737505	2,24345208	0,83842491	0,93481368	-1,98206032	3,27474356	-2,32567124	3,66122812	15,2143516	16,6370356	3,68110247	3,83551139	-23,8173832	27,2541441

Fig.3 CPIx – Threshold = 25mV

Tab 4 and Tab 5 show the statistical variance for mean values of CPI. It is evident that CPI_3 and $CPI_3|$ are the most accurate values (lower variance) for both potential thresholds.

CPIx	Variance
CPI1	11
|CPI1|	8
CPI2	4
|CPI2|	4
CPI3	2
|CPI3|	2
CPI4	10
|CPI4|	9
CPI-1	33
|CPI-1|	28
CPI-2	15
|CPI-2|	14
CPI-3	14
|CPI-3|	14
CPI-4	17
|CPI-4|	16

Tab.4 Variance of CPIx - Threshold = 70mV

CPIx	Variance
CPI1	23
|CPI1|	30
CPI2	1
|CPI2|	0,5
CPI3	0,3
|CPI3|	0,4
CPI4	2
|CPI4|	1,5
CPI-1	2
|CPI-1|	2
CPI-2	14
|CPI-2|	13
CPI-3	2
|CPI-3|	1
CPI-4	68
|CPI-4|	49

Tab.5 Variance of CPIx - Threshold = 25mV

At this point we can say that the ratio between the amount of Total Power variation and the amount of Power Above Threshold variation seems to be the main candidate for the evaluation of the effects of the perturbation of the aqueous medium of the HMC due to magnetic fields induced by different stimulation frequencies and different inputs.
Furthermore, being interested only in the magnitude of the variation, only the modulus of the perturbation ($|CPI_3|$) has been considered.

Fig.4 and 5 show trend of $|CPI_3|$ for both potential thresholds.

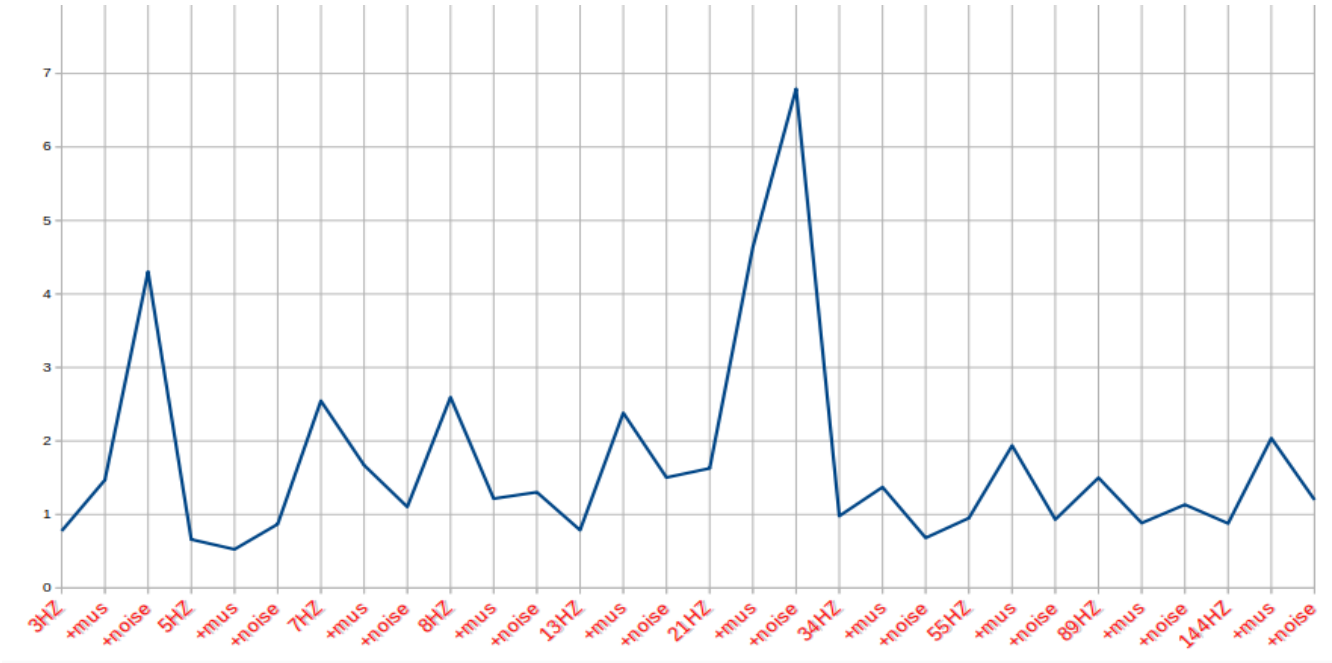

Fig.4 $|CPI_3|$ - Threshold 70mV

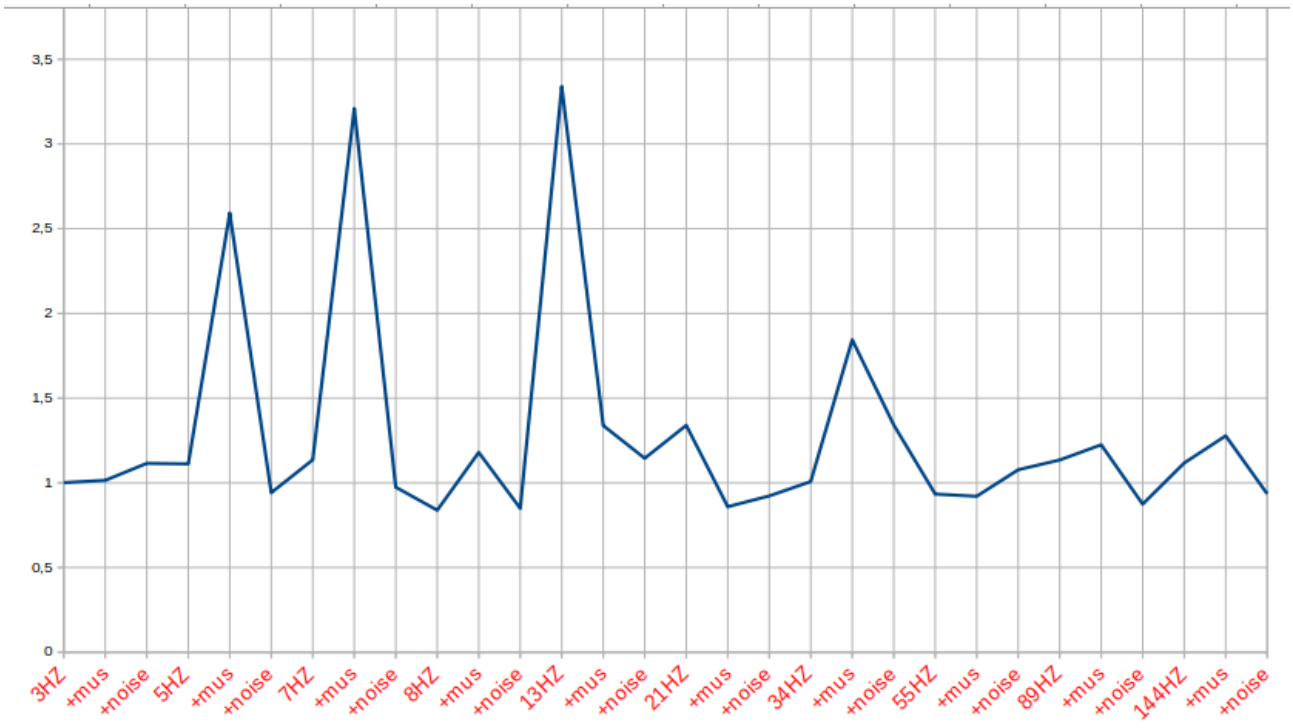

Fig.5 $|CPI_3|$ - Threshold 25mV

These graphs show that |CPI$_3$| actually has a very sensitive trend both to the stimulation frequencies and to the sensory inputs, with power peaks in delta, theta, and beta frequencies, as also predicted by the literature, and power peak variations correlated to the physical and phenomenological characteristics of the sensory input.
Nevertheless literature suggests that no emotion-*related brain activity happen at frequencies >40Hz (Farabbi et al., 2022), while |CPI$_3$| even for stimulation frequencies above 40 Hz and even >100Hz (non-physiological) shows trends similar to those obtained for frequencies in the alpha range (i.e. 8 Hz).*
According to this osevation |CPI3| still cannot be considered a rather valid index for the physical description of qualia.

C) Randomness Index
Consciousness could be interpreted as reduction of uncertainty, because every single conscious experience is one among many other possibilities, and, in mathematical terms, reduction of uncertainity is information (Shannon et al., 1999)
The effects of interaction between magnetic field and acqueous enviroment have been tested on computational ativity of the Arduino microcontroller by means of the embedded pseudo-RNG.
Tables 6 and 7 and Fig. 6 and 7 show the behavior of Deviation from Randomness (Δ) of the pseudo-RNG, in relation to stimulation frequency and sensory input.

FREQ	tRNG	Δ
3HZ	4766,62	233,38
+mus	4766,02	233,98
+noise	4923,92	76,08
5HZ	4747,7	252,3
+mus	4788,14	211,86
+noise	5009,52	-9,52
7HZ	4746,14	253,86
+mus	4754,98	245,02
+noise	4954,92	45,08
8HZ	4753,8	246,2
+mus	4754,18	245,82
+noise	4977,58	22,42
13HZ	4754,34	245,66
+mus	4754,68	245,32
+noise	4948,9	51,1
21HZ	4755	245
+mus	4755,04	244,96
+noise	4941,76	58,24
34HZ	4747,26	252,74
+mus	4748,54	251,46
+noise	4972,94	27,06
55HZ	4759,1	240,9
+mus	4719,22	280,78
+noise	4935,28	64,72
89HZ	4783,88	216,12
+mus	4799,4	200,6
+noise	5011,68	-11,68
144HZ	4863,06	136,94
+mus	4871,24	128,76
+noise	5030,68	-30,68

Tab 6: tRNG and Δ – Threshold = 70 mV

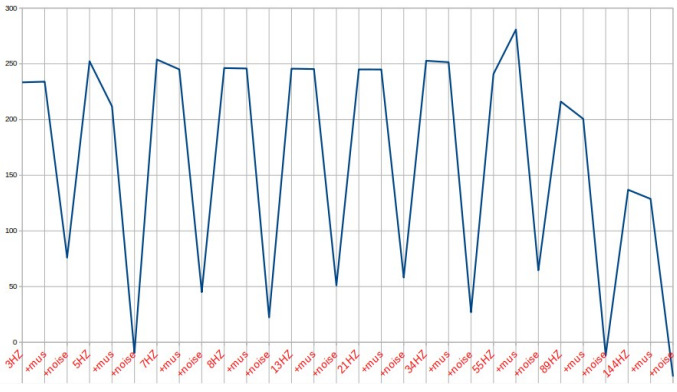

Fig.6

FREQ	tRNG	Δ
3HZ	4754,74	245,26
+mus	4744,44	255,56
+noise	4954,02	45,98
5HZ	4733,94	266,06
+mus	4737,34	262,66
+noise	4947,94	52,06
7HZ	4735,12	264,88
+mus	4730,62	269,38
+noise	4953,66	46,34
8HZ	4739,72	260,28
+mus	4736,14	263,86
+noise	4951,64	48,36
13HZ	4746,42	253,58
+mus	4735,34	264,66
+noise	4927,08	72,92
21HZ	4743,9	256,1
+mus	4754,74	245,26
+noise	4928,54	71,46
34HZ	4747,64	252,36
+mus	4758,58	241,42
+noise	4943,36	56,64
55HZ	4764,32	235,68
+mus	4772,84	227,16
+noise	4994,18	5,82
89HZ	4821,32	178,68
+mus	4819,28	180,72
+noise	4968,72	31,28
144HZ	4866,28	133,72
+mus	4865,92	134,08
+noise	5019,36	-19,36

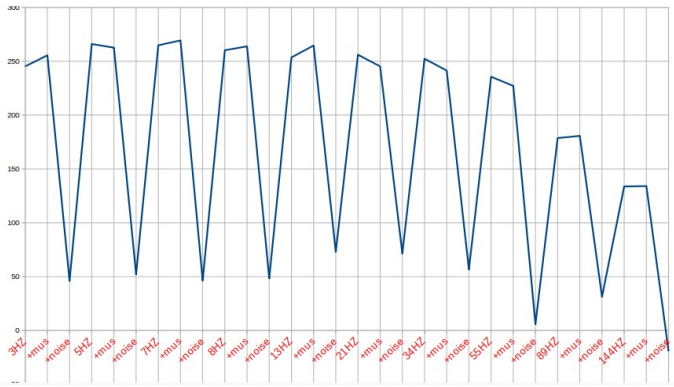

Tab 7: tRNG and Δ – Threshold = 25 mV

Fig.7

Due to the rather constant trend of tRNG and Δ, by means of the statistical significance of Δ it has been possible to group data into a Randomness Index (RI), with following values.

***a) 0** : Δ devoid of statistical significance*

***b) 0.5** : Δ p-value <.05*

***c) 1** : Δ p-value <.01*

D) Quantillium

Combining CPI_x sensitivity to the electromagnetic field with the uncertainty reduction given by the RI, a new index, called Quantillium (Ql), has been obtained.
Ql is mathematically defined by the formula:

$$Ql = CPI_x * RI$$

Fig.8 and Fig.9 show trends of the average value of each Ql obtained at the end of the 50th cycle, for each individual stimulation frequency (with and without input).

FREQ	QL	|QL|	QL2	|QL2|	QL3	|QL3|	QL4	|QL4|	QL-1	|QL-1|	QL-2	|QL-2|	QL-3	|QL-3|	QL-4	|QL-4|
3HZ	-0,74528586	1,485261326	0,688646573	1,181364517	0,222718146	0,775887074	7,077425957	9,342743053	11,65222602	16,93579026	1,25044303	5,362072737	2,256552404	4,653804476	-0,42822039	4,38327
+mus	1,450587701	2,893610782	0,413046908	1,092283367	1,185467638	1,469014366	3,189782841	4,602275184	4,911766958	8,229672514	4,554944076	5,684832293	4,322062681	5,020186146	-3,20262949	5,82902
+noise	0	0	0	0	0	0	0	0	0	0	0	0	0	0	0	
5HZ	-0,6822559	1,100477151	0,36542814	0,695402936	0,21176254	0,659564873	1,448967006	3,28066104	1,773519021	6,344211766	3,09992711	3,583207449	4,738066871	5,288418182	-3,08542079	4,74804
+mus	-0,13233646	0,610173881	0,535595991	0,82047255	0,463214019	0,525552432	-1,40346313	2,948668912	-3,55538876	5,93772049	-2,96982497	7,778530865	-7,80907977	13,43177902	10,51570828	13,0424
+noise	0	0	0	0	0	0	0	0	0	0	0	0	0	0	0	
7HZ	3,586384306	4,795064982	0,588545819	1,23223176	2,186604789	2,545540143	0,076735898	2,277381752	-0,70157793	3,964770109	0,660404172	2,455978951	1,196430835	2,408204531	0,659406179	2,20155
+mus	1,344608773	2,984542703	0,446370887	0,999857484	1,117602385	1,670295094	0,602117019	2,124512513	0,259150549	3,933281058	1,383183292	3,11000532	1,747009544	2,695626722	0,183891445	2,1155
+noise	0	0	0	0	0	0	0	0	0	0	0	0	0	0	0	
8HZ	4,323110986	5,591736893	0,483809784	1,073930943	2,290732513	2,594550804	1,14943153	1,558137094	1,285833787	2,718609724	-11,4769599	18,48342584	-8,87994522	16,25207053	11,61858133	17,4041
+mus	0,327921256	2,117393361	0,764321752	0,985785521	0,632148147	1,215490974	-1,77706859	4,964580005	-4,26535152	9,187050736	-1,49928804	5,553233491	-0,33983806	4,429636088	2,860760098	4,90300
+noise	0	0	0	0	0	0	0	0	0	0	0	0	0	0	0	
13HZ	-0,16611792	1,379030858	0,067859511	1,301646584	0,432967581	0,786762021	0,815610758	1,899786114	0,724784373	3,540255874	2,560100692	3,145460448	2,389552418	3,257754075	-0,32693312	2,89649
+mus	-3,82255782	4,631355019	0,154080157	0,960006533	-1,25965424	2,381631723	0,499304697	1,300867127	0,061553652	2,426812209	0,84767047	2,591627598	0,930813206	2,848858243	1,019508913	2,55237
+noise	0	0	0	0	0	0	0	0	0	0	0	0	0	0	0	
21HZ	1,775906824	2,935684687	0,903718402	1,480828073	1,350325455	1,627521555	-0,0825052	2,787524363	-1,021325	5,119479443	0,728164906	3,188641602	0,780574142	2,976884641	1,305852631	2,83042
+mus	-8,96405316	9,301535747	0,380718217	0,981412453	-3,65756238	4,6393595	2,936960451	4,297426123	4,675763663	8,246177043	-1,32448924	6,524859746	-1,44980699	5,913073605	3,645090286	5,75763
+noise	0	0	0	0	0	0	0	0	0	0	0	0	0	0	0	
34HZ	-0,34262041	1,567795457	0,663158392	0,870280138	0,317154977	0,979175314	0,300826482	1,807085827	-0,32849489	3,467767892	1,786278883	2,193153462	1,744988032	2,21228373	0,206351031	1,56603
+mus	1,706801477	2,293398965	0,605451733	0,658740863	1,301385859	1,371565303	0,724711755	2,653351993	0,478997555	5,144075251	2,508175131	3,055693634	3,072321455	3,546165893	-1,2049864	2,89714
+noise	0	0	0	0	0	0	0	0	0	0	0	0	0	0	0	
55HZ	0,587461783	1,609657355	0,431115564	1,207746737	0,811665979	0,95060854	-0,21622393	4,430866632	-1,23446764	8,273897107	-5,32726182	10,35623419	-1,78980954	7,127307733	3,982341469	7,08507
+mus	-0,11878384	3,765800179	0,189409037	1,515303006	0,478030471	1,936464546	-0,16607545	1,670709668	-1,14558763	2,881859674	0,141373863	2,889239455	-0,04160624	3,281758522	2,509266372	3,79510
+noise	0	0	0	0	0	0	0	0	0	0	0	0	0	0	0	
89HZ	2,237149089	3,32398426	-0,28162958	1,702629395	1,416464962	1,499283047	11,49825066	13,85499282	17,50734126	22,12933196	-4,94840594	11,22941095	-4,54911501	10,39287375	8,478495058	14,4257
+mus	-0,51437108	1,910248441	0,925798298	1,469316062	0,4350204	0,883589122	0,277976386	1,753244671	-0,20331361	2,87274429	3,283380098	4,042480481	3,840727838	5,187625854	-4,01896975	7,93296
+noise	0	0	0	0	0	0	0	0	0	0	0	0	0	0	0	
144HZ	0	0	0	0	0	0	0	0	0	0	0	0	0	0	0	0
+mus	0	0	0	0	0	0	0	0	0	0	0	0	0	0	0	
+noise	0	0	0	0	0	0	0	0	0	0	0	0	0	0	0	

Fig.8 Ql – Threshold = 70mV

FREQ	QL	|QL|	QL2	|QL2|	QL3	|QL3|	QL4	|QL4|	QL-1	|QL-1|	QL-2	|QL-2|	QL-3	|QL-3|	QL-4	|QL-4|
3HZ	-0,89909367	3,81590066	0,2967453	1,57667544	0,78066485	1,0011158	-0,39631588	1,25282696	-0,59281085	1,44714648	0,35463298	2,78556924	1,03499115	1,55121172	0,74771956	5,97590256
+mus	1,04851665	3,65600282	-0,94704157	2,25844207	0,99716504	1,01457154	-1,43877335	2,98228417	-1,77433599	3,42344221	-6,20146834	11,2699973	0,68131367	2,26756091	4,08393378	11,375412
+noise	0	0	0	0	0	0	0	0	0	0	0	0	0	0	0	0
5HZ	-0,01553692	4,5526965	1,37812567	1,78464881	0,92005323	1,11163275	-1,46401326	2,98300372	-1,79219198	3,38779008	0,48474354	2,10366178	0,90944865	1,46253144	1,6624788	5,65023543
+mus	-12,4784052	16,3653925	0,71446667	1,60448651	-0,42500515	2,59213936	3,42966365	4,23054165	3,76729049	4,8068171	0,63909089	1,72241884	0,94861554	1,16123927	1,38929179	3,67453654
+noise	0	0	0	0	0	0	0	0	0	0	0	0	0	0	0	0
7HZ	-0,59782452	4,32367195	1,35091149	1,55808664	0,81293191	1,13553117	0,12517733	1,65789084	0,00865944	1,88962229	0,66726908	1,4064627	0,94561908	1,1149226	1,46855429	2,98741076
+mus	5,882383	23,350572	0,80780607	1,38350601	1,51140623	3,2091552	0,02419255	1,32694912	-0,1021397	1,50520438	0,81725579	2,16685625	0,95970136	1,35215889	1,15529942	5,42765029
+noise	0	0	0	0	0	0	0	0	0	0	0	0	0	0	0	0
8HZ	-0,21907023	1,58425793	1,5459676	1,85606373	0,83800175	0,83800175	-0,72083178	4,13425573	-0,98686599	4,8046384	1,43212819	1,45412063	1,48752093	1,48752093	-2,3220246	3,35618348
+mus	-0,22653851	5,50920026	-0,03934545	1,51734769	0,77635168	1,17951972	0,01661591	1,85392136	-0,11519634	2,0926202	2,46452465	4,43251328	1,21851498	2,03429362	-0,71257331	10,8590538
+noise	0	0	0	0	0	0	0	0	0	0	0	0	0	0	0	0
13HZ	-20,2358789	22,0357637	0,43761538	1,64220388	-1,47478174	3,3392407	0,31158766	1,232869	0,20989537	1,38700251	1,21076352	1,32462486	1,12934087	1,16840365	0,1814387	2,60860638
+mus	-0,87073375	6,11302725	1,06491167	1,56495472	0,76455585	1,33802209	1,13355894	4,52097767	1,15686691	5,1678176	1,43334031	2,43601915	1,47588068	1,88220688	-2,802562	7,89735184
+noise	0	0	0	0	0	0	0	0	0	0	0	0	0	0	0	0
21HZ	3,70351253	4,93869917	0,6414432	1,42611985	1,33939647	1,33939647	0,47172784	1,66086797	0,39731778	1,90117503	1,07258893	1,38788711	1,15913555	1,15913555	-0,09407539	2,25984332
+mus	-0,92794598	2,07545524	1,05614092	1,09087203	0,77151214	0,8587838	1,49665438	3,71489761	1,58412028	4,26353627	2,79472911	3,02130639	2,42475134	2,73381393	-8,13636167	12,3405693
+noise	0	0	0	0	0	0	0	0	0	0	0	0	0	0	0	0
34HZ	1,06353475	3,12886129	1,16400621	1,24810388	1,0015144	1,00723836	0,64140819	1,80730416	0,59481305	2,07895516	1,68395874	1,93839314	1,62336316	1,91441543	-3,58161458	7,43258084
+mus	0,41846409	9,72670549	-1,50695587	3,77417848	0,9125243	1,84423354	1,5727945	3,20722706	1,66019185	3,64444524	-0,27220664	2,23291093	0,51056801	1,73835226	4,09477712	6,82871466
+noise	0	0	0	0	0	0	0	0	0	0	0	0	0	0	0	0
55HZ	-2,59411257	4,0708226	0,3911791	1,76588594	0,54348381	0,93346325	-0,12491328	3,03227149	-0,27684108	3,44011927	-1,74032416	3,38242865	1,03370269	1,94034013	0,36994003	9,15543362
+mus	-0,18330363	1,80287989	1,30603845	1,81830148	0,87068727	0,92030006	-2,26847971	3,38485932	-2,67275212	3,80907934	0,85047885	0,93155679	0,77832827	1,35879091	2,60653142	3,78415187
+noise	0	0	0	0	0	0	0	0	0	0	0	0	0	0	0	0
89HZ	-0,9	2,7	0,08	1,1	0,35	0,55	0	0,4	0,06	0,5	0,5	1	0,5	0,6	0,25	2,2
+mus	1,2	2,7	1,2	1,35	0,7	0,6	0	1	0	1	0,8	2,3	0,6	0,6	0,6	2,25
+noise	0	0	0	0	0	0	0	0	0	0	0	0	0	0	0	0
144HZ	0	0	0	0	0	0	0	0	0	0	0	0	0	0	0	0
+mus	0	0	0	0	0	0	0	0	0	0	0	0	0	0	0	0
+noise	0	0	0	0	0	0	0	0	0	0	0	0	0	0	0	0

Fig.9 Ql – Threshold = 25mV

Tab 8 and Tab 9 show the statistical variance for all mean values of Ql.
As for CPI it is evident that Ql_3 and $|Ql_3|$ are the most accurate values (lower variance) for both potential thresholds.

Ql	Variance
Ql	5
|Ql|	5
QL_2	4
$\|QL_2\|$	4
QL_3	1
$\|QL_3\|$	1
QL_4	6
$\|QL_4\|$	9
QL_{-1}	17
$\|QL_{-1}\|$	26
QL_{-2}	9,5
$\|QL_{-2}\|$	17
QL_{-3}	9
$\|QL_{-3}\|$	16
QL_{-4}	12,5
$\|QL_{-4}\|$	20

Tab.8 Ql Variance - Threshold = 70mV

Ql	Variance
Ql	11
|Ql|	8
QL_2	4
$\|QL_2\|$	4
QL_3	2
$\|QL_3\|$	2
QL_4	10
$\|QL_4\|$	9
QL_{-1}	33
$\|QL_{-1}\|$	28
QL_{-2}	15
$\|QL_{-2}\|$	14
QL_{-3}	14
$\|QL_{-3}\|$	14
QL_{-4}	17
$\|QL_{-4}\|$	16

Tab.9 Ql Variance - Threshold = 70mV

Since it has been decided to analyze only the magnitude of the perturbation of the system, also in this case only the behavior of |Ql3| has been analyzed.

Fig.10 and 11 show trend of $|Ql_3|$ for both potential thresholds.

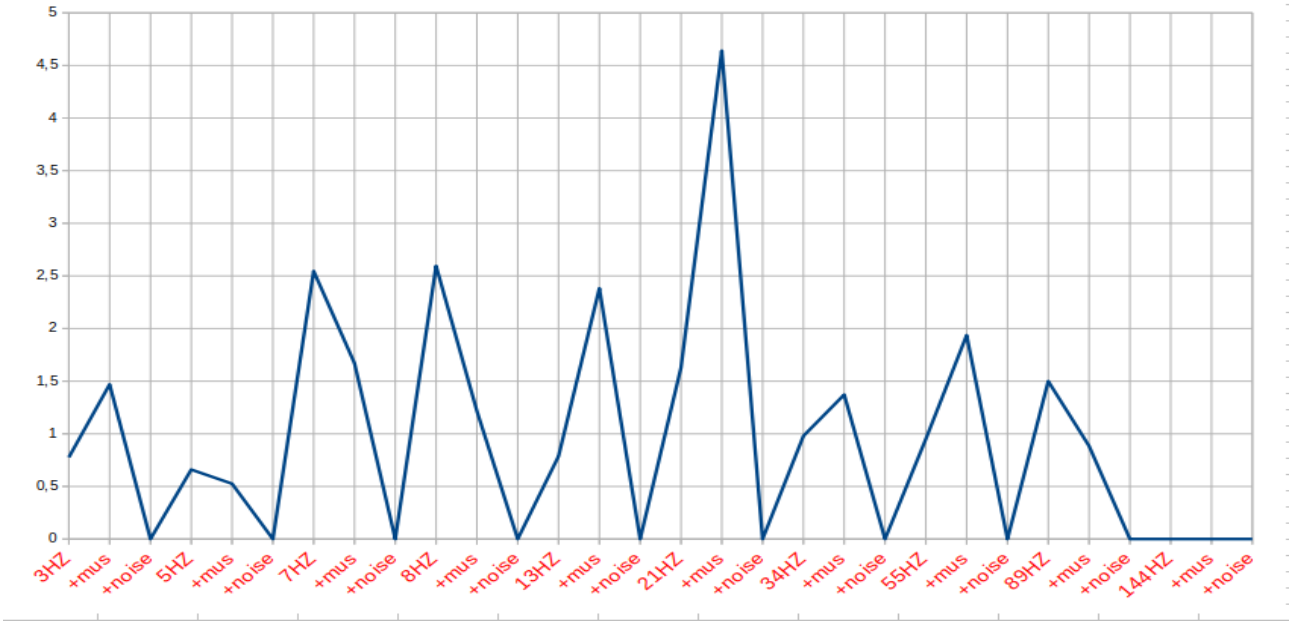

Fig.10 $|Ql_3|$ - Threshold 70mV

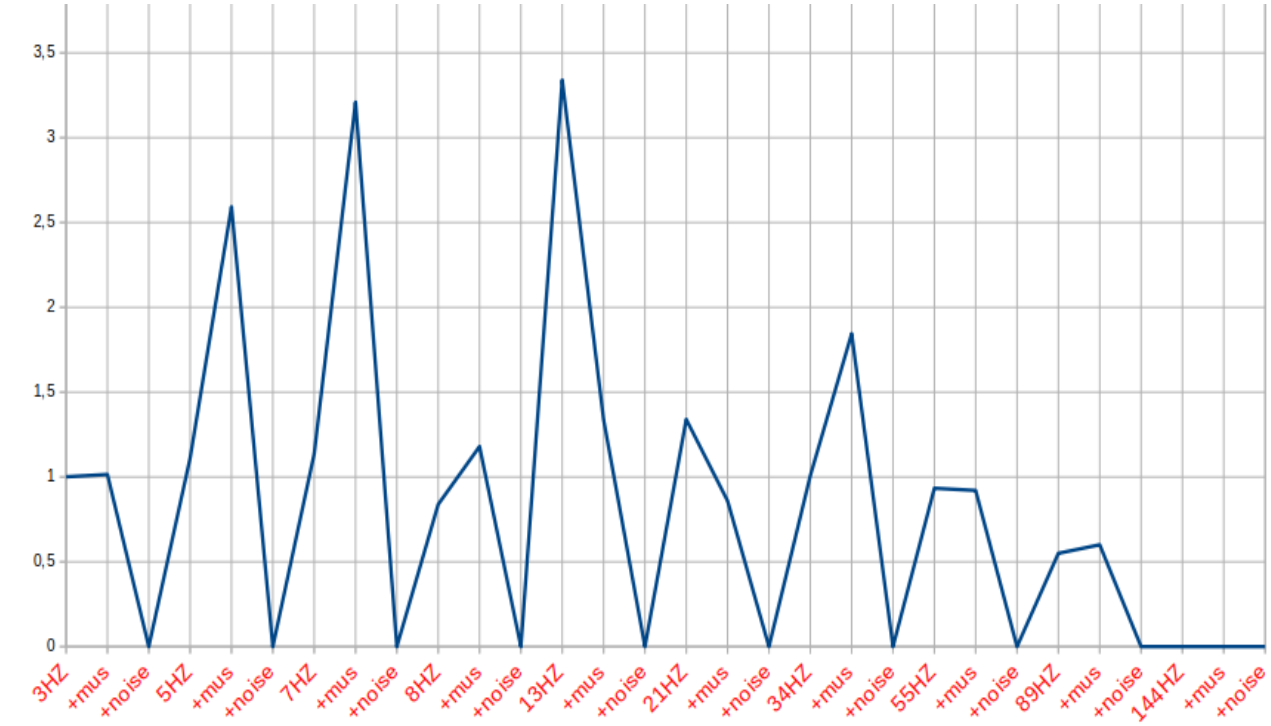

Fig.11 $|Ql_3|$ - Threshold 25mV

It is noteworthy that the behaviour of the Ql, compared to that of the CPI, actually shows lower power peaks for stimulation frequencies >40Hz (especially for potential threshold at 25mV) and no power peaks for non-physiological frequencies (>100Hz).
Ql thus becomes a much more reliable index of HMC environment perturbation by sensory inputs of different kinds and can considered a good indicator of the phenomenological aspects of conscious experiences (qualia).

Discussion

Vicinal water is the main constituent of every living brain. Interactions between vicinal water and brain waves activity could be at the origin of an emergent property, called Causal Power, postulated by John Searle, that could solve the notorious hard problem of David Chalmers: how can rise subjective experience from a physical structure of any complexity?
Results presented in this work show that interactions between water and magnetic fields oscillating with frequency <40Hz range can repesent the singularity from which qualitative perception of stimuli from the external environment (qualia) arise.
Furthermore this perception can be measured by means of an index called Quantillium (Ql).
But i*t is noteworthy* that Ql can be defined only for analog inputs, while neurons could be considered as digital structures: they can assume only two configurations, on-off, from which inhibitory or excitatory behaviors follow (Debanne et al., 2013).
So, how can discrete neuronal activity be embedded in a HMC-like system and how can qualia originate from it?
In this regard two kinds of approach can be postulated: a biophysical one and an architectural one.

a) Biophysical Approach
According to Cavaglia' et al *(Cavaglia' et al., 2023)* during action potentials neuronal membrane dipole generated by the phospholipid head groups, coherent dipole oscillations can be formed. Under suitable conditions these dipolar oscillations, interacting with their neighbors, become synchronized, with a plausible Froehlich mechanism of biological coherence, and generate EMFs (according to Maxwell Theory of electromagnetism), leading to signals propagation both into the cellular interior and in the inter-cellular network (see fig.12).
Coherent EMF produced by dipole oscillations in the membrane of one neuron can indcuce constructive or destructive interference pattern with similar EMFs produced by neighboring neurons, creating a hologram interference pattern and offering the plausibility of 3D holographic image formation, as previously proposed by Pribram with the Holonomic Brain Theory (Pribram et al., 1986), containing analog information about sensory input that trigger neuronal activity.
This model is actually consistent with two main theories of mind: the Integration Information Theory *(Tononi, 2017) a*nd McFadden's Electomagnetic Information Field Theory *(McFadden, 2020).*
Finally this approach could be demonstrated by clinical evidence and experimentally validated with quantum optomechanics techniques.

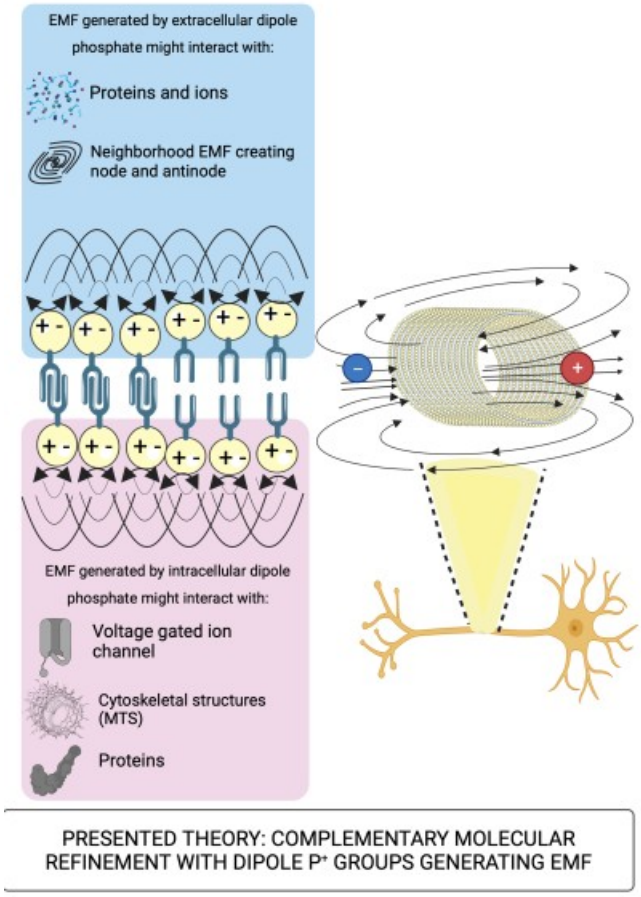

Fig.12 (reprinted from Cavaglia' et al,2023)

b) Architectural approach
Connections between neurons can develop in various ways, like that shown in Fig. 13:

Fig.13: a simple scheme of connections between neurons (reprinted from Pribram, 1991)

Each neuron, according to Hogkin-Huxley model, is characterized by its own electrical resistance, varying from 10^4 to 10^9 ohm depending on whether the fibers are non-myelinated or myelinated. The previous image can then be simplified as follow (Fig. 14):

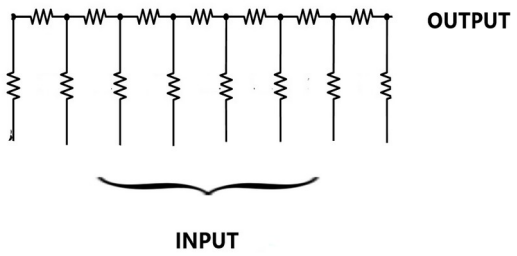

Fig.14: a simple scheme of connections between neurons with electric resistance

This scheme is very similar to a peculiar electronic circuit, called R-ladder, that actually is a digital analog converter (DAC; Fig. 15)(Kester, 2009).

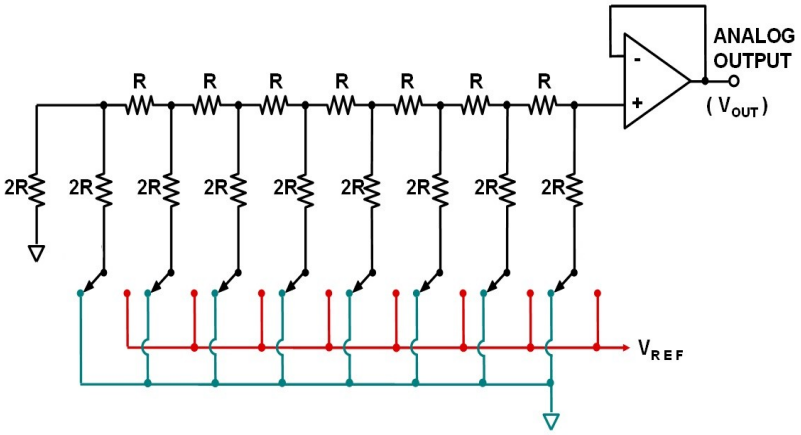

Fig.15: DAC scheme

This hypothesis, unlike that described for the biophysical approach, cannot be subjected to experimental and clinical verification, but Arduino technology has allowed the realization of an 8-bit R2R ladder which has been subsequently integrated into the HMC system (Fig.16 – Sketch 2 in Appendix 1)

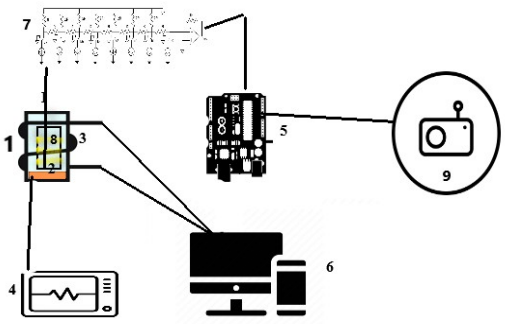

Fig.16

According to this experimental set-up, the sensory input to the aqueous core of the HMC is no longer provided by direct connection between the internal stimulation coil and the audio player, but by the R2R DAC (7) inserted at the output of the microcontroller. In this case the audio impulse (9) is fed into the Arduino (5) through an analog pin, converted into a set of digital signals (as in fact the brain neurons would do) and subsequently reconverted, by the 8-bit neuronal system, in an analog signal which is then sent to the core through the internal stimulation coil (8).
The analog signal that has been converted to a digital signal, thanks to the action of R2R, could become analog again and reach the core, allowing evaluation of Ql and phenomenological perception of the input.
Furthermore, if we introduce a feedback system, where output of coil 3 is sent not only to the PC but also to the microcontroller (Fig.17 red lines), we get a strong amplification of the analog input (in this case audio input)(Fig.18 and Fig.19).

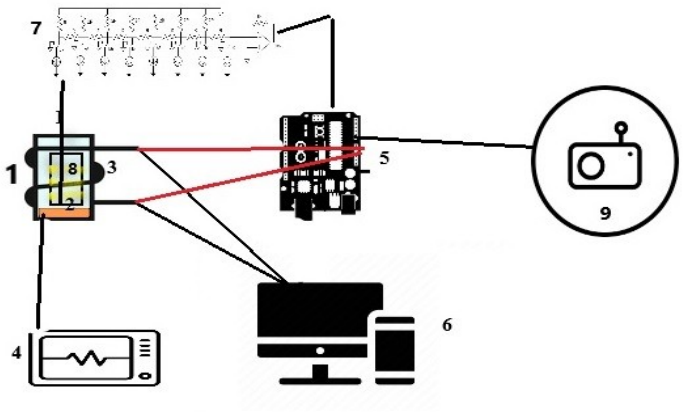

Fig.17: HMC with DAC and feedback

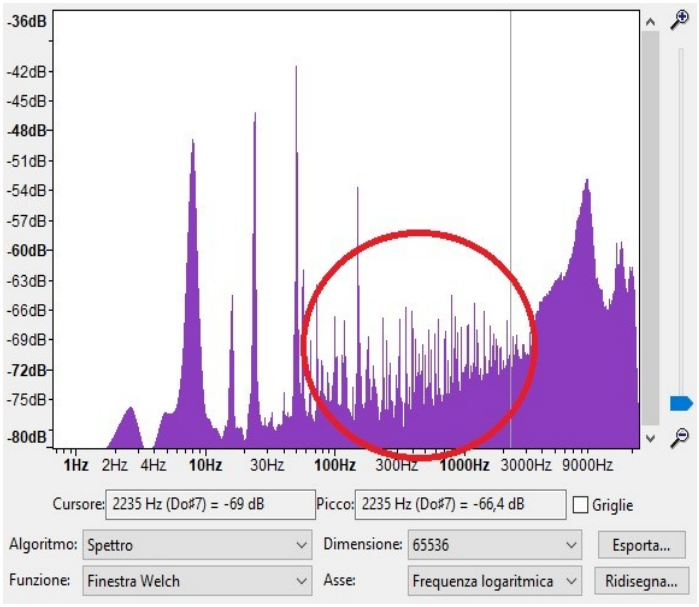

Fig.18: R-ladder without feedback

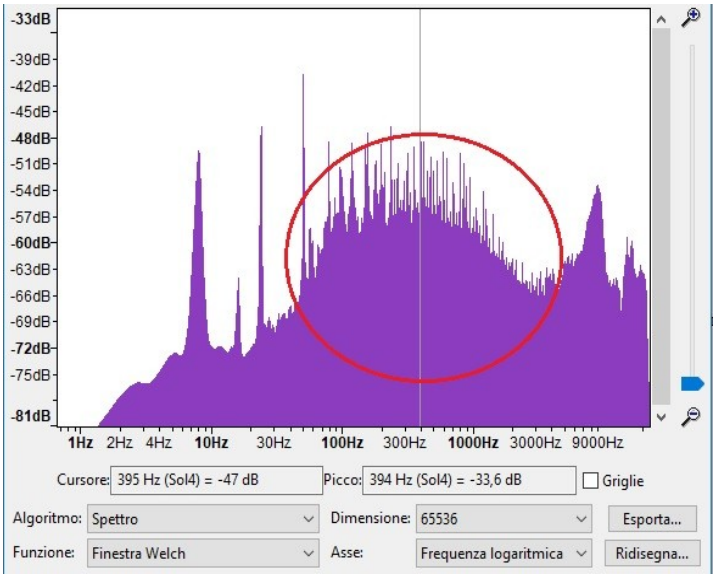

Fig.19: R-ladder with feedback

Obviously the poor computational power of the microcontroller used in our experimental model (10 bits) allows a rather poor processing of the audio input, but we could imagine the effects of a high computational power like that of human cerebral cortex made up of billions of interconnected neuronal cells.

Conclusions

Compared to other theoretical studies this work deals with the development of an artificial setup (HMC) that could be useful for the experimental investigation of a new paradigm of neuroscience, where interactions between water and magnetic fields, not neurons, are the cradle of conscious experience and subjectivity.
Neurons and neuronal networks constitute the information decoding hardware. This decoding is mostly digital, but passive properties of the neuronal cells and their interconnections allow for a digital-to-analog reconversion of the signal. This analog signal is probably responsible for the transmission of information to the aqueous environment and for the perception, during waking state, of stream of consciousness and semantic experiences.
In agreement with results of this study, from a biophysical point of view, “qualia” can be defined as the amplitude of perturbation of the cerebral aqueous medium by coherent magnetic fields and magnetic field induced by neuronal networks activity under various conditions of stimulation from the external environment.
Since the activity of the HMC involves both the integration of information embedded in the magnetic fields activity and the deviation from pure randomness of the behavior of the computational element, it can be argued that Quantillium is consistent with IIT.
Furthermore Ql trend is strictly dependent also on the different excitability of the aqueous medium (represented by Potential threshold) and this fact could be a plausible explanation of individual variability of phenomenological experiences.
Finally HMC technology is very cheap and experiments reported in present work are reproducible and therefore falsifiable (according to Popper's principle), with any kind of analog input, frequency stimulation and Potential threshold.
In the next future HMC technology could be embedded in weighted artificial neural network, maybe leading to the creation of a new kind of Artificial Intelligence. But, are we really sure we want it?

Data availability statement

All Data and results presented in the study are included in article or in supplementary material. Further inquiries can be directed to the corresponding author.

Funding

The author declare that no financial support was received for the research, autorship, and/or publiation of this article.

Acknowledgements

The author thanks Carlino Luigi for the creation of the original term “Quantillium”.

Conflict of interest

The author declare that the research was conducte in the absence of any commercial or financial relationships that could be construed as a potential conflict of interest.

References

1) Cavaglia', M., Deriu, M.A., Tuszynski, J.A. (2023).Toward a holographic brain paradigm: a lipid-centric model of brain functioning. Front. Neurosci. 17: 1302519. DOI=10.3389/fnins.2023.1302519.

2) Chalmers, David J. (1996). The Conscious Mind: In Search of a Fundamental Theory (2nd edition). Oxford University Press.

3) Debanne D, Bialowas A, Rama S.(2013). What are the mechanisms for analogue and digital signalling in the brain? Nat Rev Neurosci. Jan;14(1):63-9. doi: 10.1038/nrn3361. Epub 2012 Nov 28. PMID: 23187813.

4) Farabbi, A., Polo, EM., Barbieri, R., Mainardi, L.(2022) Comparison of different emotion stimulation modalities: an EEG signal analysis. 44th Annual International Conference of the IEEE Engineering in Medicine & Biology Society (EMBC), Glasgow, Scotland, United Kingdom, 2022, pp. 3710-3713, doi: 10.1109/EMBC48229.2022.9871725.

5) John ER. (2002). The neurophysics of consciousness. Brain Res Brain Res Rev. Jun;39(1):1-28. doi: 10.1016/s0165-0173(02)00142-x. PMID: 12086706.

6) Kester, W. (2009). "MT-014 Tutorial: Basic DAC Architectures I: String DACs and Thermometer (Fully Decoded) DACs" (PDF). Analog Devices. Archived (PDF) from the original on 2023-03-13. Retrieved 2023-07-06.

7) Kester, W. (2009). "MT-015 Tutorial: Basic DAC Architectures II: Binary DACs" (PDF). Analog Devices. Archived (PDF) from the original on 2022-10-06. Retrieved 2023-06-26.

8) McFadden, J. (2020). Integrating information in the brain's EM field: the cemi field theory of consciousness. Neurosci Conscious. 2020, 1–13. doi: 10.1093/NC/NIAA016

9) Nagel, Thomas (1974). What is it like to be a bat? Philosophical Review 83 (October):435-50.

10) Pollack, G.H. (2013). The Fourth Phase of Water. Ebner and Sons

11) Pribram KH, Carlton EH. (1986). Holonomic brain theory in imaging and object perception. Acta Psychol (Amst). Dec;63(1-3):175-210. doi: 10.1016/0001-6918(86)90062-4. PMID: 3591432.

12) Pribram K (1991). Brain and Perception. Hillsdale: Lawrence Erlbaum

13) Shannon, Claude E. & Weaver, Warren (1949). The Mathematical Theory of Communication. University of Illinois Press.

14) Tononi, G. (2017). The integrated information theory of consciousness: an outline. Blackwell Companion to Conscious. 11, 243–256. doi: 10.1002/9781119132363.CH17

15) Wahbeh, H., Radin, D., Cannard, C., Delorme, A.(2022) What if consciousness is not an emergent property of the brain? Observational and empirical challenges to materialistic models. Front Psychol. Sep 7;13:955594. doi: 10.3389/fpsyg.2022.955594. PMID: 36160593; PMCID: PMC9490228.

16) Warfield, T. A. (1999). Searle's causal powers. Analysis 59 (1):29-32.

17) Zeman, A. (2001). Consciousness. Brain: A Journal of Neurology, 124(7), 1263–1289. https://doi.org/10.1093/brain/124.7.1263

APPENDIX 1

Arduino Sketches

SKETCH 1: S-POT, TP, PAT, PBT, tRNG, Δ

```
void(* resetFunc) (void) = 0;
long x = 0;
long somma = 0;
long sommaI = 0;
long sommaC = 0;
int tot=0;
int scarto;
void setup() {
  Serial.begin(9600);
}
void loop(){
for(x; x <10000; x++){
int B = analogRead (A0);
int H = B;
int I = B;
if (B > 14){    //This value control the potential threshold (each unit corresponds to 5 mV; so 5 =
                  25mV and 14=70mV)
int  C = B;
sommaC = sommaC + C; //            PAT
B = 1;
}
else{
  B = 0;
}
randomSeed(H);
int W=random(2);
tot = tot + W; //                  tRNG
somma = somma + B; //              S-POT
sommaI = sommaI + I; //            TP
scarto=5000-tot; //                Δ
delay (1);
}
Serial.print(somma); Serial.print(" "); Serial.print(sommaI); Serial.print(" ");
Serial.print(sommaC); Serial.print(" "); Serial.print(sommaI - sommaC); Serial.print(" ");
Serial.print(tot); Serial.print(" "); Serial.print(scarto); Serial.println(" ");


delay (100);

resetFunc();
}
```

SKETCH 2: R-Ladder (with two inputs)

```
void setup() {
  for (byte i=0;i<8;i++){
    pinMode(i,OUTPUT);
  }

}

void loop() {
  int A = analogRead(A0);
  int B = analogRead(A2);
  int C = (A + B +1)/4 - 1;
  if (C < 0){
    C = 0;
  }
PORTD = C;
                                                    }
```